

# Equivalent Charge Source Model Based Iterative Maximum Neighbor Weight for Sparse EEG Source Localization

PENG XU,<sup>1,2</sup> YIN TIAN,<sup>1,3</sup> XU LEI,<sup>1</sup> XIAO HU,<sup>2</sup> and DEZHONG YAO<sup>1</sup>

<sup>1</sup>Center of Neuroinformatics, School of Life Science and Technology, University of Electronic Science and Technology of China, ChengDu 610054, China; <sup>2</sup>Department of Neurosurgery, Neural Systems and Dynamics Laboratory, The David Geffen School of Medicine, University of California, Los Angeles 90095, USA; and <sup>3</sup>College of Bio-Information, ChongQing University of Posts and Telecommunications, ChongQing 400065, China

(Received 13 April 2008; accepted 18 September 2008)

**Abstract**—How to localize the neural electric activities within brain effectively and precisely from the scalp electroencephalogram (EEG) recordings is a critical issue for current study in clinical neurology and cognitive neuroscience. In this paper, based on the charge source model and the iterative re-weighted strategy, proposed is a new maximum neighbor weight based iterative sparse source imaging method, termed as CMOSS (Charge source model based Maximum neighbor weight Sparse Solution). Different from the weight used in focal underdetermined system solver (FOCUSS) where the weight for each point in the discrete solution space is independently updated in iterations, the new designed weight for each point in each iteration is determined by the source solution of the last iteration at both the point and its neighbors. Using such a new weight, the next iteration may have a bigger chance to rectify the local source location bias existed in the previous iteration solution. The simulation studies with comparison to FOCUSS and LORETA for various source configurations were conducted on a realistic 3-shell head model, and the results confirmed the validation of CMOSS for sparse EEG source localization. Finally, CMOSS was applied to localize sources elicited in a visual stimuli experiment, and the result was consistent with those source areas involved in visual processing reported in previous studies.

**Keywords**—EEG source imaging, Inverse problem, Weighted minimum norm solution, Charge source model, Weight matrix, Neighbor source information.

## INTRODUCTION

The scalp electroencephalogram (EEG) represents electrical activity manifested by the ensemble of a great number of neurons within the brain. Estimating the location and distribution of the underlying equivalent electric generators based on the scalp EEG is the EEG

inverse problem.<sup>16</sup> Presently, the activated areas are usually simulated or approximated with some electromagnetic model. The equivalent dipole,<sup>12,19,27</sup> the equivalent charge and the local field potential are the three currently adopted source models, and among these three models, the charge model is promising for its simpler expression, wider adaptivity and smaller computation complexity for EEG inverse problem when compared with other two source models for many situations.<sup>7,10,11,32,33,36</sup> In this paper, the inverse problem is expressed and solved based on the charge source model, and the algorithm has the similar procedure when the other two kinds of source models are considered for inverse problem, where the only difference is the lead field matrix constructed with different sources.

The general EEG inverse problem with an assumption of a few unknown focal activated areas is essentially a non-linear optimization problem. To simplify the EEG inverse problem, the complex non-linear problem is sometimes realized by a linear approach, which is usually based on the distributed source assumption that the solution space consists of all the possible source positions.<sup>11,16,22,28,30,31,33</sup> Mathematically, such a linear approach can be stated as,

$$Y = AX + \varepsilon \quad (1)$$

where  $Y$  is the scalp EEG recordings of  $M \times 1$ ,  $M$  is the number of scalp electrodes.  $A$  is the lead field matrix of  $M \times N$  with  $N$  being the dimension size of the discrete solution space.  $X$  is the source solution vector to be estimated and  $\varepsilon$  is the noise induced in the recording. For EEG inverse problem,  $M$  is usually much smaller than  $N$ , which means that the system is underdetermined, thus the problem lacks a unique solution because there are an infinite number of possible source configurations that could explain the measured recordings  $Y$ . To obtain a physiologically feasible solution, some possible and reasonable

Address correspondence to Dezhong Yao, Center of Neuroinformatics, School of Life Science and Technology, University of Electronic Science and Technology of China, ChengDu 610054, China. Electronic mail: dyao@uestc.edu.cn

constraints are necessary, such as the minimum norm least square solution (MNS) developed in the early effort.<sup>9,30</sup> However MNS favors the superficial source, that is to say, for a deep source, the localized source will have some bias toward the scalp surface. The popularly adopted one is the weighted minimum norm solution (WMNS), among which the low-resolution electromagnetic tomography (LORETA) is the mostly used due to its robust imaging ability to the extended sources, though its result is really blurring, and LORETA solution is often used the initialization distribution for such some iterative procedures as FOCUSS. Many researchers are still making great efforts to improve the spatial resolution of EEG localization methods to satisfy the requirements of neurological research.<sup>15,16,20,21,34</sup>

The difficulty to solve EEG inverse problem is somewhat due to the seriously underdetermined characteristics of matrix  $A$  with much more unknown variables than the observed ones, thus another way to improve the solving of the EEG inverse problem is to use source model with fewer freedoms to lower the dimension of matrix  $A$ , i.e., reduce the unknown variables. Currently, dipoles normal to cortex surface are used to map activations on cortex, and these radial dipoles are useful when activations are mainly on the superficial cortex, whereas some deep brain areas have been found to be involved in such complex cognitive processes as inhibition of return (IOR).<sup>24,25</sup> Apparently, the cortex radial dipoles are not competitive for such cognitive researches. Alternatively, other source models such as the charge model and the local field potential model are newly developed to image brain activations, both of them are of just one unknown variable (freedom) for one source point compared to three when dipole is used for the general EEG inverse problem,<sup>7,16,33</sup> therefore using the charge source model or local field potential model will lower the dimension of the inverse problem and improve the performance of the lead field matrix, and thus the solving will be much easier and more efficient compared with the dipole model. (Certainly, when some special dipoles such as radial dipoles on cortex surface are used, the dipole freedom can be reduced to one, too.) In Yao *et al.*,<sup>32,33</sup> the authors developed algorithms based on charge source model to estimate the electrical activities of brain. The authors also discussed the difference between charge model and dipole model in detail, and confirmed that the charge model is feasible for the localization of the brain activities.<sup>33,36</sup> Alternatively, in Grave de Peralta Menendez *et al.*,<sup>7</sup> the authors developed the method based on potential to estimate activated brain areas, too.

To solve this underdetermined system, sparsity of source distribution has been used as another constraint

imposed to EEG inverse problem.<sup>4,15,16,28,31</sup> Presently, there are three approaches to get sparse solution for EEG inverse problem. In the source localization approach developed in early studies, a few sources were prior supposed, and then a non-linear optimization method was taken to solve the inverse problem, which is usually called the dipole fitting approach. The second way was to directly solve the  $l_p$  ( $p \leq 1$ ) norm solution of the inverse problem, such as the  $l_1$  norm solution.<sup>28</sup> In recent years, the methods based on solution space shrinking were emphasized. Starting with an initial blurring distributed source solution, such as MNS and LORETA, by iteratively shrinking the solution space, the solution would converge to a relatively sparse one, including the self-coherence enhancement algorithm (SCEA)<sup>34</sup> and the focal underdetermined system solver (FOCUSS),<sup>3-6,17,31</sup> etc. FOCUSS is a repeated WMN procedure with the weighting matrix constructed from the source strengths in previous iteration, and it recursively adjusts the weighting matrix until most elements of the solution become nearly zero, thus achieving a sparse solution.

However, the final solution of FOCUSS largely depends on the initial source distribution,<sup>22</sup> and various studies confirmed that FOCUSS is sensitive to source configurations to some degree,<sup>16,17</sup> i.e., for some special source configurations, FOCUSS cannot recovery the sources as desired. Current efforts in improvement of FOCUSS are mainly paid to improve the calculation of the matrix inverse and various techniques such as singular value decomposition (SVD) truncation and other regularization techniques are adopted to deal with noise.<sup>6,16,17,31</sup>

The weight matrix adopted in FOCUSS is based on the source distribution estimated in the prior iteration. According to FOCUSS weighting strategy, the stronger source is estimated on one solution point in the last iteration, the larger weight will be imposed on the corresponding solution position in the next iteration, thus in the following iterations, these strong sources will be usually enhanced and simultaneously sources in other solution positions will be easily degraded. Such a strong-source enhancement strategy made it difficult for FOCUSS to modify the possible solution bias induced in the previous iterations and the bias will be unexpectedly passed down to the following iterations, and we think this weight drawback may be somewhat overcome with the aiding of the neighboring source information. In fact, in the initial source distribution provided by those methods such as LORETA and MNS to FOCUSS, bias is unavoidable when true sources are sparsely distributed, and the source position is quite possible to be wrongly estimated on some other neighbored point. Therefore, all those positions in the neighbor instead of only the position having

strongest power could be the possible source candidate locations in one iteration, and we need to impose large enough weights on those possible source positions to improve their competitive ability to compete with the current strongest position in the next iteration to modify the bias, and the method developed in this paper is designed in this way to improve the source localization ability.

In this work, we defined a new weight matrix by utilizing the neighboring source information in the last iteration, and then the new weight is integrated into an iterative procedure like FOCUSS to iteratively solve the EEG inverse problem with the charge source model. For convenience to describe the approach in the paper, the new weighting iterative method is termed as Charge source model based *Maximum neighbor weight Sparse Solution* (CMOSS). The method was introduced in section “Methods.” The adopted head model and lead field were described in section “Head model.” In section “Simulation test,” the algorithm was tested and compared with FOCUSS and LORETA on a realistic 3-shell head model for various source configurations. Finally, the new method was applied to localize the sources elicited in an exogenous visual stimulus experiment in section “Real data test.” Discussions and conclusions concluded this paper.

## METHODS

### *Charge Source Model and Forward Calculation*

The popularly used source model in EEG inverse problem is the dipole model, and the charge model is a relatively new one for EEG imaging.<sup>32,33,36</sup> In fact, the theory of brain electric field shows us that the potential  $\Phi$  generated by neural electrical activities in an infinite homogeneous head model can be stated as,<sup>35</sup>

$$\begin{aligned}\Phi &= -\frac{1}{4\pi\sigma} \int_V \left(\frac{1}{r}\right) \nabla \cdot \vec{J}_S dv = \frac{1}{4\pi\sigma} \int_V \nabla \left(\frac{1}{r}\right) \cdot \vec{J}_S dv \\ \nabla \cdot \vec{J}_S(\vec{r}) &= I_F(\vec{r}) \\ \Phi &= -\frac{1}{4\pi\sigma} \int_V \left(\frac{1}{r}\right) I_F dv\end{aligned}\quad (2)$$

where  $\sigma$  is the conductivity,  $\vec{J}_S$  is the primary current density distribution of neurons,  $I_F$  is the divergence of the current density usually termed as current source density. The first equation shows that  $\vec{J}_S$  behaves like a dipole, and the third equation shows that  $I_F$  behaves like a charge, thus Eq. (2) shows us that both charge and dipole can generate the same potential, and they are theoretically related to each other. In essence, both of

them are equivalent source models approximating to the complex actual physiological neural activities,<sup>35,36</sup> and between them, a dipole may be considered as an equivalent representation of a pair of closely neighboring positive and negative charges. As compared with dipole, the number of unknown variables to be estimated when using charge model is only 1/3 of that when using dipole model without radial orientation or other constraints imposed, and the reduction of unknown variables (freedom) can lower the computation complexity and improve the characteristic of lead matrix, which will avail for the stable solving of the inverse problem. In this paper, we used the charge source model to image the source activations, and some further explanations of the difference between charge model and dipole model can be found in literatures.<sup>32,33,35,36</sup>

In this work, the forward calculation for the complex realistic head model is conducted with Boundary Elements Method (BEM).<sup>1,2</sup> The only difference for BEM between dipole and charge is to use the charge potential field (the third formula in Eq. 2) instead of the dipole potential field (the first formula in Eq. 2) in the standard BEM approach.

### *Weighted Minimum Norm Solution*

#### *Strategy of the Weighted Minimum Norm*

The weighted minimum norm solution is the mostly adopted algorithm in current EEG inverse problem. With weight matrix  $W$ , the weighted form of EEG inverse problem is,

$$\begin{aligned}Y &= AX + \varepsilon = AWW^+X + \varepsilon = Dq + \varepsilon, \text{ with} \\ X &= Wq, D = AW\end{aligned}\quad (3)$$

where  $q$  is an auxiliary variable. The weighted minimum-norm solution of the inverse problem is,

$$\hat{X} = W^{-1}A^T[AW^{-1}A^T]^+Y \quad (4)$$

where  $[AW^{-1}A^T]^+$  denotes the Moore–Penrose pseudo-inverse of  $[AW^{-1}A^T]$ . The weight matrix  $W$  greatly affects the solution of inverse problem and in the following sections, the Laplacian and iterative weights that can estimate the sources extensively or sparsely will be introduced.

#### *Laplacian Weighted Minimum Norm Solution*

The widely adopted Laplacian weighted matrix  $W$  in EEG inverse problem has the form as,

$$W = BG, \text{ with } G = \text{diag}(\|a_1\|, \|a_2\|, \dots, \|a_N\|) \quad (5)$$

where  $B$  denotes the discrete spatial Laplacian operator;  $\|a_i\|$  is the  $i$ th column norm of the lead field matrix  $A$ .<sup>22</sup> The solution with such weight strategy is the low

resolution electromagnetic tomography (LORETA) and the solution of LORETA is extensive and blurring. The corresponding LORETA based on charge source model, i.e. cLORETA, was developed by Yao and He, and the difference of sources localized with these two source models was discussed in Refs. 11,33.

#### Iterative Re-Weighted Minimum Norm Solution

Different from the LORETA weight strategy, the weight of the re-weighted minimum norm solution is iteratively constructed with the solution during the iterations. The weight matrix  $W_k$  in the  $k$ th iteration is constructed by the prior iteration solution  $X_{k-1}$  as,

$$W_k = (\text{diag}(X_{k-1})) \quad (6)$$

With this weight, the inverse problem can be solved with a sparse and focal solution and the iterative solving procedure based on this weight strategy is named the focal underdetermined system solver (FOCUSS) by Gorodnitsky.<sup>4-6</sup> In practice, FOCUSS is implemented with the following three steps:

1.  $W_k = (\text{diag}(X_{k-1}))$
2.  $q_k = (AW_k)^+ Y$
3.  $X_k = W_k q_k$

The initial source distribution  $X_0$  is usually provided by LORETA at the beginning of the iteration procedure. One FOCUSS procedure needs to repeat the above three steps for several times, when the iteration number is above the predefined maximum iteration number or the difference between the neighboring iterations is smaller than the termination tolerance error, the iteration will be terminated and a sparse and energy localized solution will be achieved.

Similar to that of cLORETA, when the lead field matrix  $A$  is calculated with the charge source model, the Charge FOCUSS (cFOCUSS) can be easily developed.

#### Iterative Maximum Neighbor Weight Sparse Solution

##### The Iterative Maximum Neighbor Weight

In the  $k$ th iteration of FOCUSS, the object function can be represented as,

$$\min_{X_k} \|W_k^+ X_k\|^2 = \min_{X_k} \|q_k\|^2 = \min_{X_k} \sum_{i=1, w_{kii} \neq 0}^N \left( \frac{x_{ki}}{w_{kii}} \right)^2 \quad (8)$$

where  $w_{kii}$  is the  $i$ th diagonal element of  $W_k$ , and  $x_{ki}$  is the  $i$ th element of  $X_k$ . The above equation shows that a large weight can lower the contribution of those sources at the corresponding spatial position to the object function, and therefore avails for the estimation of a source with strength  $x_{ki}$  at those positions in sense

of the minimum norm solution. As the weights of FOCUSS are directly constructed with the sources estimated in the last iteration, the FOCUSS iteration procedure will favor to enhance those spatial positions with strong sources estimated in the previous iteration, and simultaneously the sources on those positions with weak strength will be easily iteratively degraded, thus when the strength difference between the strong source and weak source is too remarkable, in view of minimum sense denoted by Eq. (8), those positions with very weak sources estimated in the prior iteration are not able to compete with those positions having strong sources in prior iteration. Apparently, with such a weighting way, if the initial or previous estimation has spatial bias, it is not easy for FOCUSS to modify the bias effectively in the following iterations due to the neglect of the neighbor information, and may finally result in a biased source distribution.<sup>15</sup>

In each iteration of the FOCUSS procedure, it is quite possible to wrongly localize the sources on other position close to the actual source position, and in the FOCUSS weighting strategy, FOCUSS may fail to modify this bias due to a relatively weak weights imposed on the actual solution points in the following iterations, and if this bias is not rectified in the next iteration in time, this bias may expand. Alternatively, we can construct a weight not just using the solution of the point itself but also combing the information of the neighbor points to modify the possible solution bias during iterations. By considering the sources in neighbors, we defined a new diagonal weighting matrix  $W_N$  with its  $i$ th diagonal element  $w_{Nii}$  being,

$$w_{Nii} = \begin{cases} \sqrt{\max(|x_j|, x_j \in \Omega_i) \times x_i, x_i > 0} \\ -\sqrt{\max(|x_j|, x_j \in \Omega_i) \times |x_i|, x_i \leq 0} \end{cases}, 1 \leq i \leq N \quad (9)$$

where  $\Omega_i$  is the 26-neighbor domain of the  $i$ th point in the discrete solution space. With the weighting matrix  $W_N$ , the weighted form of inverse problem is similar to that in Eq. (3) as,

$$Y = AX = AW_N W_N^+ X \quad (10)$$

In matrix  $W_N$ , if the strongest source within neighbor is located on current neighbor center, the weight is the current source strength, which is similar to the FOCUSS weight; however, when the strongest source is not located at the neighbor center, the weight is enhanced compared to that used in FOCUSS. Apparently, the main difference between these two weight strategies is in the case when the strongest source is not located at the neighbor center. For this case, the FOCUSS strategy will impose a weaker

weight on this spatial position, and the source at this position is easy to be degraded in the consecutive FOCUSS iterations, thus if this position is the actual source position, FOCUSS may localize a source on other position close to the true position with certain bias or even lose it; however, with the new construction strategy, those weights may be enhanced and emphasized by the neighboring strong sources so that the contrast between the large weight and small weight will be lowered in one neighbor. As stated by the object function in Eq. (8) that the large weight avails for the estimation of sources at the corresponding solution points, so the enhanced weights can provide more chance for iteration procedure to modify the source bias induced in the former iterations.

During the first several iterations, the estimated sources are distributed on many points in the discrete solution space, and accordingly there may have several sources in a neighbor, thus the enhancement of weight is obvious. With the iteration on, the source distribution becomes sparse with many null entries existing in the solution space, therefore the weights constructed in these iterations are not easy to be enhanced and are very similar to FOCUSS weight, which can guarantee the convergence of CMOSS.

Besides, such regularization techniques as singular value truncation can be adopted to deal with the effect of noise contaminated in signal.<sup>6,17,29</sup>

#### Procedure of CMOSS

The CMOSS can be realized with the following iteration procedure:

1. Preparation. Find and store the 26 neighbors of each point in the discrete solution space according to Euclidian distance measure; Calculate the charge lead field matrix  $A$ .
2. Initialization. Set  $k = 1$ ; set iteration termination error  $\varepsilon$  and maximum iteration number  $T_{\max}$ ; initialize source distribution  $X_{k-1}$  with cLORETA solution.
3. Update the diagonal weight matrix  $W_{Nk}$  according to formula (9).
4. Estimate the value of the auxiliary variable  $q_k$ :  $q_k = (AW_{Nk})^+ Y$ .
5. Update source distribution:  $X_k = W_k q_k$ .
6. Judge the termination condition. Compare the difference between the current and the last source distribution, if  $\|X_k - X_{k-1}\| \leq \varepsilon$  or  $k \geq T_{\max}$ , terminate the iteration and  $X_k$  is the final source distribution; else  $k = k + 1$ , and jump to step 3 and go on.

Though the procedure is described with the charge source model, it is easy to extend this weight strategy

to the dipole source model or local field potential model only by using the corresponding lead field matrix to replace the charge source lead field matrix.

## HEAD MODEL

A 3-shell realistic head model is used for EEG source localization, whose conductivities for cortex, skull and scalp are 1.0, 1/80 and  $1.0 \Omega^{-1} \text{m}^{-1}$ , respectively.<sup>26</sup> The solution space is restricted to cortical gray matter, hippocampus and other possible source activity areas, consisting of 910 cubic mesh voxels with 10 mm inter-distance. The number of vertices on brain, skull and scalp surfaces are 1514, 605 and 1219, and the corresponding numbers of the triangles on brain, skull and scalp surfaces are 3024, 1206 and 2434, respectively. The 128 electrodes were registered to the scalp surface, and the meshes and electrodes are shown in Fig. 1. When using BEM to calculate the potential of electrodes, we regarded the potential on the vertex closest to the electrode as the potential of the corresponding electrode. The lead field matrix  $A$  is calculated with charge model by BEM<sup>2</sup> for the 128 electrode system and it is a matrix with dimension of  $128 \times 910$ . The origin of the coordinate system is defined as the mid-point between the left and right pre-auriculars, and the directed line from the origin through the nasion defines the  $+X$ -axis, the  $+Y$ -axis is the directed line from the origin through the left pre-auricular. Finally, the  $+Z$ -axis is the line from the origin toward the top of the head (through electrode Cz). In all of the results reported, the maximum iteration number  $T_{\max}$  for cFOCUSS and CMOSS is 50 for both, and the tolerance error  $\varepsilon$  is 1.0E-6 for both of them.

## SIMULATION TEST

### Localization for Different Source Configurations

The localization methods were greatly affected by the source configurations, i.e., source number, source

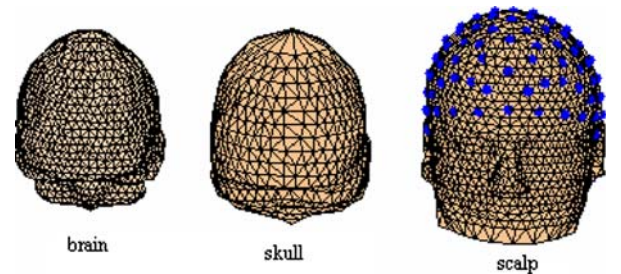


FIGURE 1. Meshes of the realistic head model for BEM. The blue points are the electrodes on the scalp.

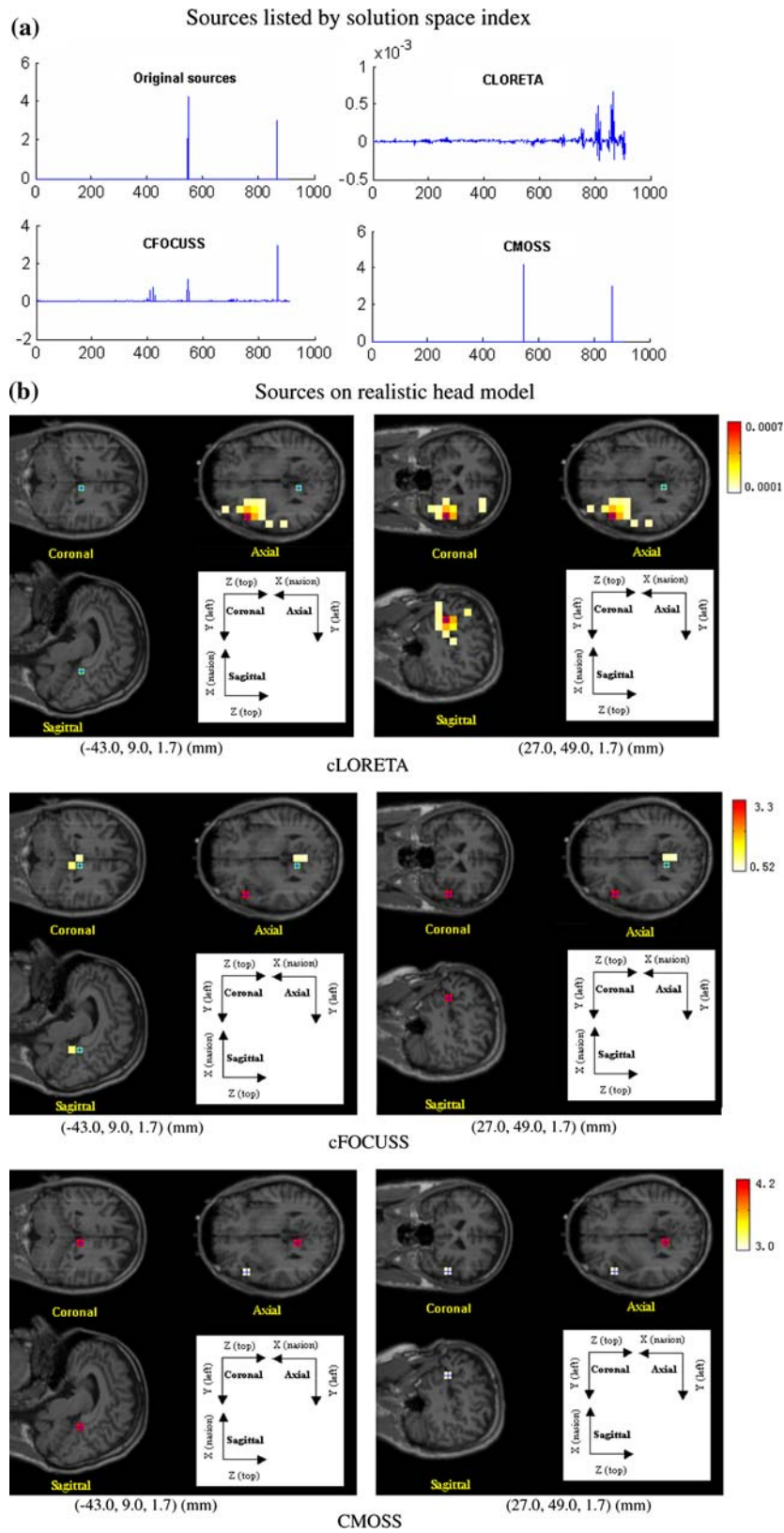


FIGURE 2. Localization for configuration with two sources. Colorful rectangle area in (b) is the estimated source location; the blue cross line within the colorful rectangle indicates the overlapping area of the simulated source and the estimated source; the blue cross line within green circle indicates those simulated source locations that are not overlapped with the positions of the estimated sources.

position, etc.<sup>8,16</sup> In the following simulations, three different source configurations containing some deep sources were selected to test the localization performance of cLORETA, cFOCUSS and CMOSS, respectively.

#### Configuration with Two Sources

Two charge sources with strengths of 4.2 and 3.0 were placed at two isolated positions  $(-43.0, 9.0, 1.7)$  (mm) and  $(27.0, 49.0, 1.7)$  (mm), where source 1 was a deep source. The scalp potentials were obtained by BEM. cLORETA, cFOCUSS and CMOSS were taken for source localization. The localization results are shown in Fig. 2.

#### Configuration with Three Sources

In this simulation, three charge sources with strengths of 6.0, 4.0 and 3.9 were placed at three isolated positions  $(7.0, -21.0, 71.7)$  (mm),  $(-13.0, -11.0, 51.7)$  (mm) and  $(67.0, 19.0, 11.7)$  (mm), among which the first and the third were two superficial sources and the second one was a deep source. The scalp potentials were generated by BEM, too. cLORETA, cFOCUSS and CMOSS were also used to localize the three sources. The localization results are shown in Fig. 3.

To analyse the effect of the new weight matrix on the source estimation in the iterations, the source information in the 6 cFOCUSS iterations and in the 6 iterations of CMOSS are shown in Fig. 4, respectively.

#### Configuration with Four Sources

In this simulation, four charge sources with strengths 2.3, 4.2, 3.0 and  $-5.8$  were placed at four isolated positions  $(-53.0, -11.0, -18.3)$  (mm),  $(6.7, 9.0, -8.3)$  (mm),  $(-13.0, 29.0, -28.3)$  (mm) and  $(-53.0, 59.0, 21.7)$  (mm), with the former three sources deeply located and the fourth one superficially located. The localization results are shown in Fig. 5.

#### Localization Under Noise

In this simulation, we used the above configuration with three sources to simply test the effect of noise on these three EEG inverse methods. In this paper, Noise-to-signal-ratio (NSR) is used to represent the noise level, and NSR is defined as the ratio between the power of noise and that of signal. As EEG inverse problem is usually sensitive to noise, and 5% limitation has been suggested for actual problem,<sup>23</sup> the simulated scalp potentials were contaminated with 5 and 10% white Gaussian noise. The localization results of cLORETA, cFOCUSS and CMOSS with 5 and 10% noise are shown in Fig. 6. For the 5% noise case, the SVD truncation thresholds for cLORETA, cFOCUSS and CMOSS are 0.03, 0.05 and 0.05, respectively; for 10% noise case, the SVD truncation thresholds were set to be 0.08, 0.1 and 0.1, respectively.

#### Statistical Features of the Localization Methods

Generally, the head model, source position and the source configuration etc affect the performance of a

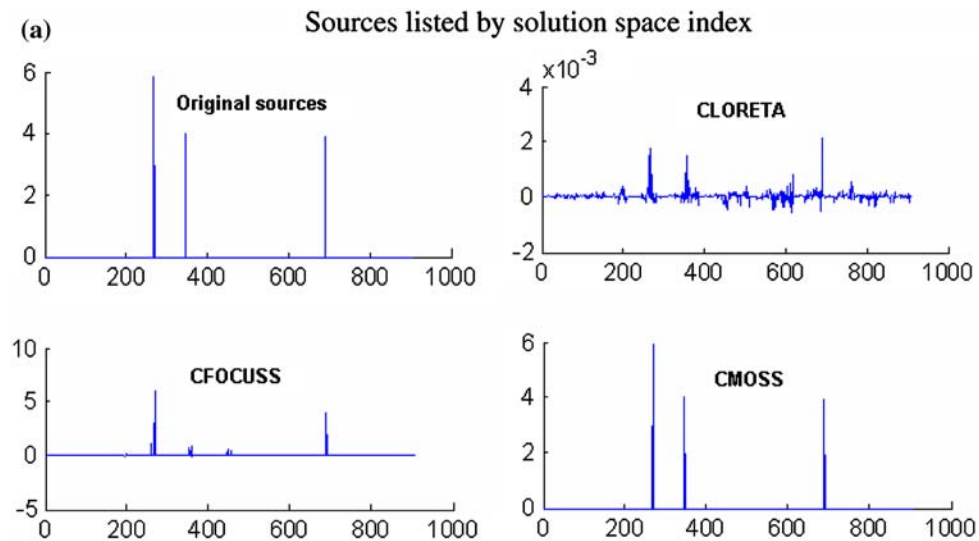


**FIGURE 3.** Localization for configuration with three sources. Colorful rectangle area in (b) is the estimated source location; the blue cross line within the colorful rectangle area indicates the overlapping area of the simulated source and the estimated source; the blue cross line within green circle indicates those simulated source locations that are not overlapped with the positions of the estimated sources.

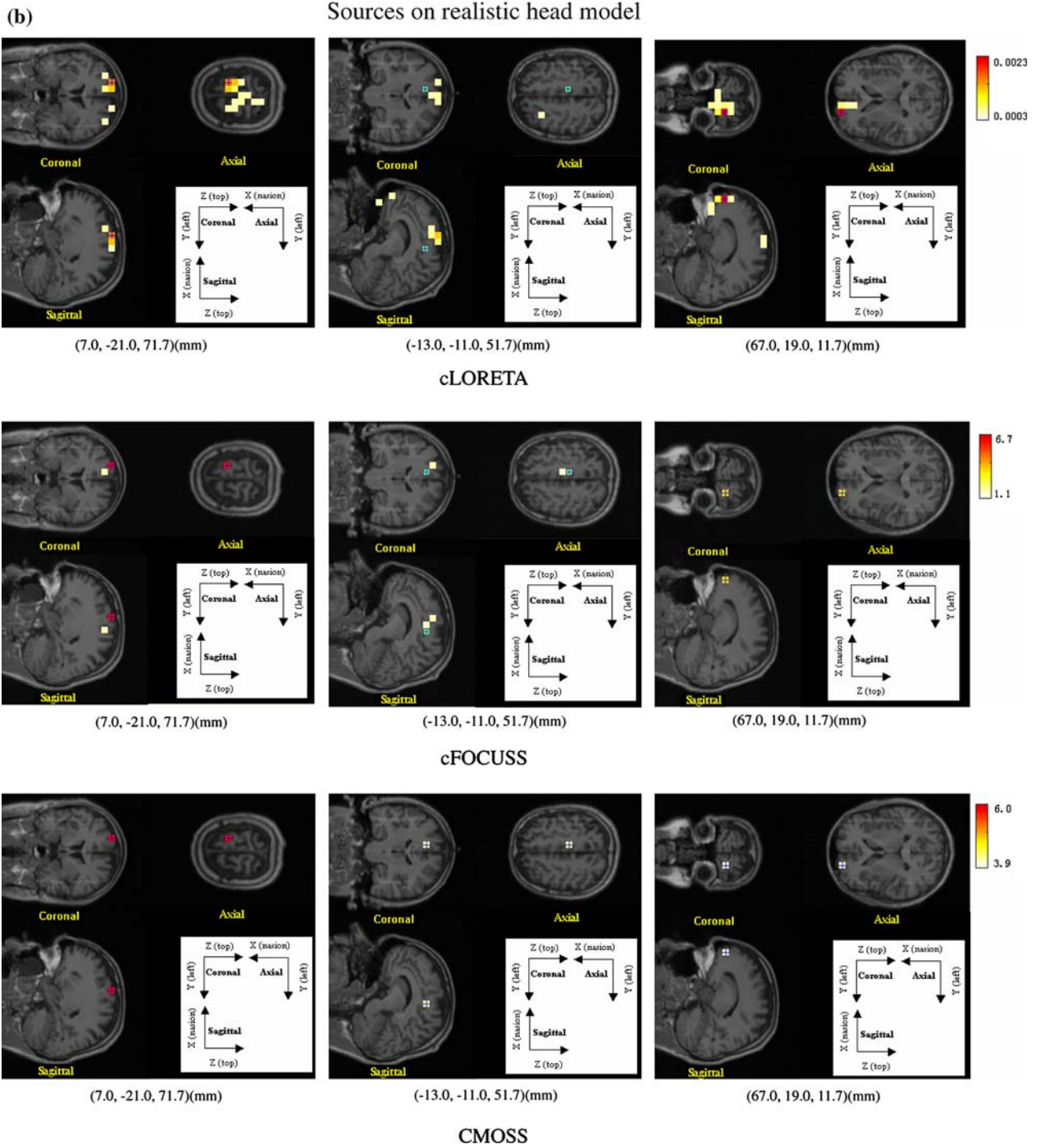
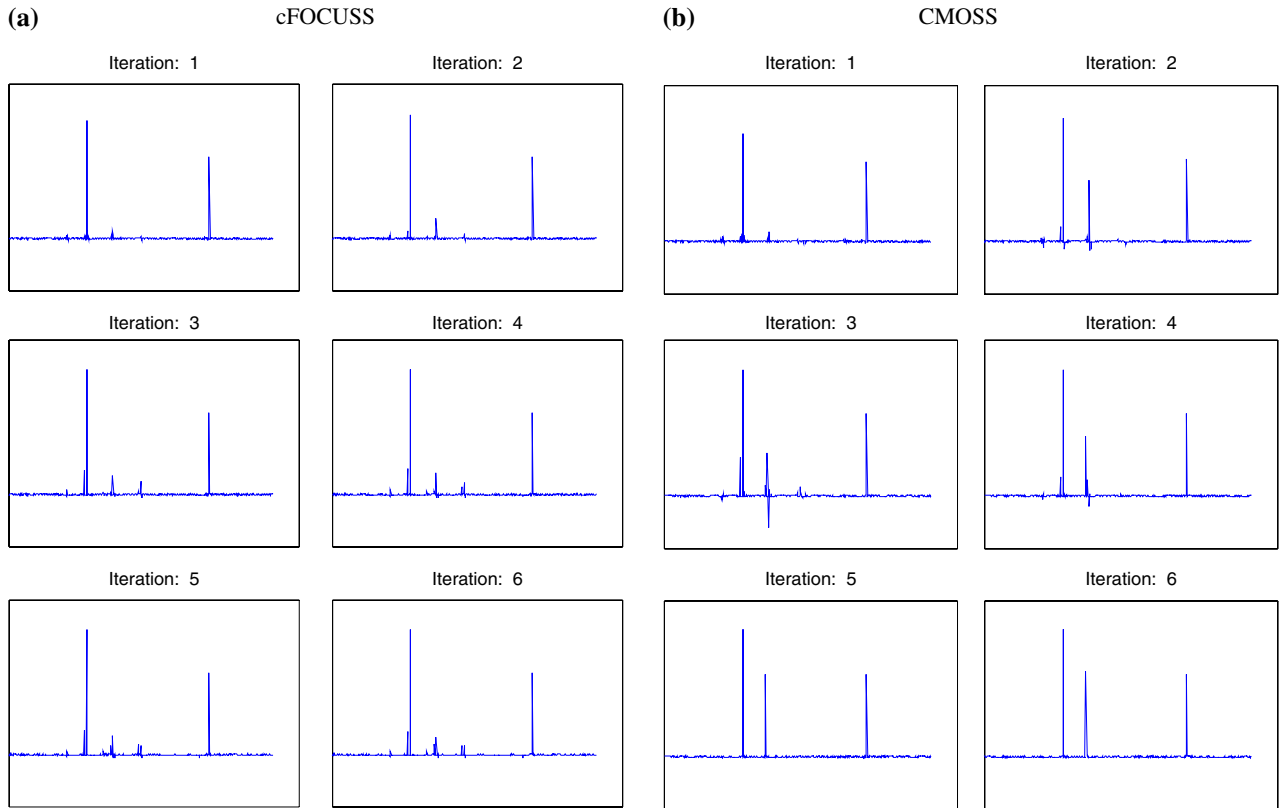


FIGURE 3. continued.

localization algorithm. Position error and strength error are two criteria to quantitatively evaluate the EEG localization algorithm.<sup>15,16,31</sup> The localization position error is defined as  $E_{\text{localization}} = \|p_{\text{est}} - p_{\text{simu}}\|$ , where  $p_{\text{est}}$  and  $p_{\text{simu}}$  are the position vectors of the estimated source and the desired (simulated) source; the strength error is defined as  $E_{\text{energy}} = \frac{\|J_{\text{simu}} - J_{\text{est}}\|}{\|J_{\text{simu}}\|} \times 100\%$ ,

where  $J_{\text{est}}$  and  $J_{\text{simu}}$  are strengths of the estimated source and the assumed (simulation) source, respectively. For the one source case, the source with the maximum power is usually regarded as the estimated source,<sup>8</sup> and if more sources are used it is not easy to correctly assign the estimated sources to the corresponding simulated sources one by one. In this



**FIGURE 4. The sources estimated in 6 iterations for cFOCUSS and CMOSS: (a) 6 iterations for cFOCUSS; (b) 6 iterations for CMOSS.**

simulation, by placing unit source on each solution node,  $E_{\text{localization}}$  and  $E_{\text{energy}}$  were calculated for each node with 10% noise considered, and then the mean and standard deviation (SD) of  $E_{\text{localization}}$  and  $E_{\text{energy}}$  were calculated over the 910 cases. Apparently, a small  $E_{\text{localization}}$  and  $E_{\text{energy}}$  were expected for a good localization method when configuration consists of point-like sources.

After  $E_{\text{localization}}$ ,  $E_{\text{energy}}$  were evaluated on each position, the mean and SD of errors were calculated over all the 910 cases for the three methods. The two indices are shown in Fig. 7. SVD truncation thresholds were set to be 0.08, 0.1 and 0.1 for cLORETA, cFOCUSS and CMOSS, respectively.

## REAL DATA TEST

### *Exogenous Visual Stimulus Experiment*

Twelve subjects (22–30 years of age) participated in the experiment. All had normal or corrected-to-normal vision and were naive with regard to the purpose of the experiment. The subjects were paid for the experiment.

The experiment followed a typical exogenous visual paradigm. A fixation cross ( $0.5^\circ \times 0.5^\circ$ ) was presented

at the center of the monitor, with a standard EGI's keyboard composed of four keys side by side. The target stimulus with a bar ( $0.50^\circ \times 0.25^\circ$ ) appeared with equal probability in the left visual field (LVF) or right visual field (RVF), with its center  $5^\circ$  off and  $2.5^\circ$  above the fixation cross. Each trial began with the presentation of a fixation point (a duration of 700 ms). And then the target was presented for duration of 200 ms. The intertrial interval (ITI) ranged randomly between 1200 and 1400 ms.

Subjects were required to fixate at the cross and minimize eye blinks and body motion as possible during all the stimulus blocks. They were instructed to press the key with their right thumb if the target stimulus appeared. Response accuracy and speed were emphasized equally. The experiment consisted of a total of 800 trials for each participant, separated into five blocks with each of 160 trials. Short breaks were allowed between blocks.

The EEG was recorded with the EGI 128-channel EEG recording system (Electrical Geodesics, Inc., 2003). The vertex electrode was used as reference for recording and the recordings were re-referenced to average offline. The bandpass was set to 0.1–40 Hz; the sampling rate was 250 Hz (4-ms samples); and all impedances was kept below 5 k $\Omega$  by moistening a

sponge with saline and placing it between the skull and electrode.<sup>18</sup> The continuous EEG was segmented into an epoch starting 200 ms before the onset of the stimulus and lasting until 800 ms after the stimulus onset. EEGs were averaged separately for all combinations of conditions (visual field: left vs. right) over the 1000 ms epoch. Individual trials with excessive muscle activities, eye movements, or blink artifacts were excluded. The grand average of the epochs for the

left target stimuli is shown in Fig. 8. The peak at 176 ms elicited by visual stimulus was used for source localization.

*Sources of Visual Stimuli Localized with CMOSS*

With CMOSS, the activated areas at 176 ms responding to visual stimuli are shown in Fig. 9 where SVD truncation threshold used for CMOSS was 0.1.

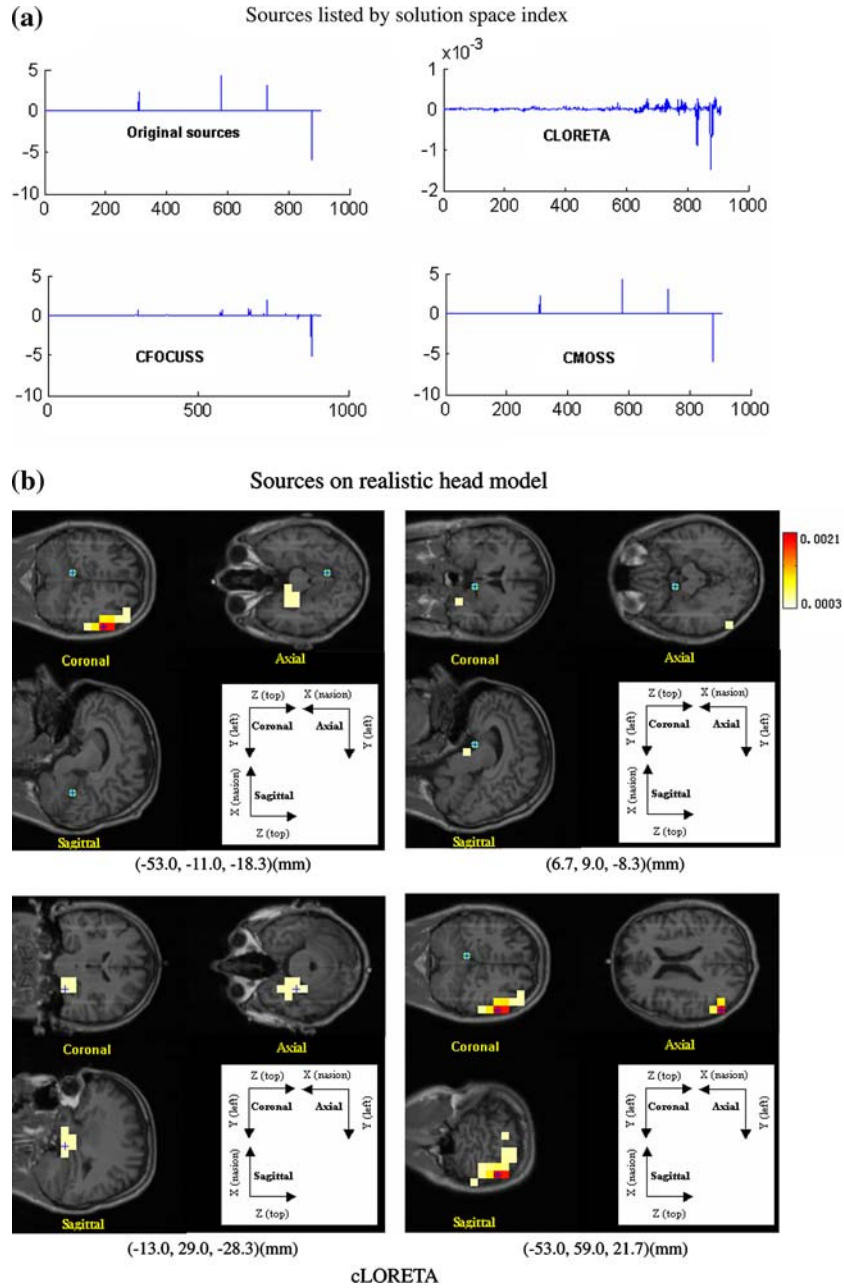


FIGURE 5. Localization for configuration with four sources. Colorful rectangle area in (b) is the estimated source location; the blue cross line within the colorful rectangle area indicates the overlapping area of the simulated source and the estimated source; the blue cross line within green circle indicates those simulated source locations that are not overlapped with the positions of the estimated sources.

Equivalent Charge Source Model Based Iterative Maximum Neighbor Weight

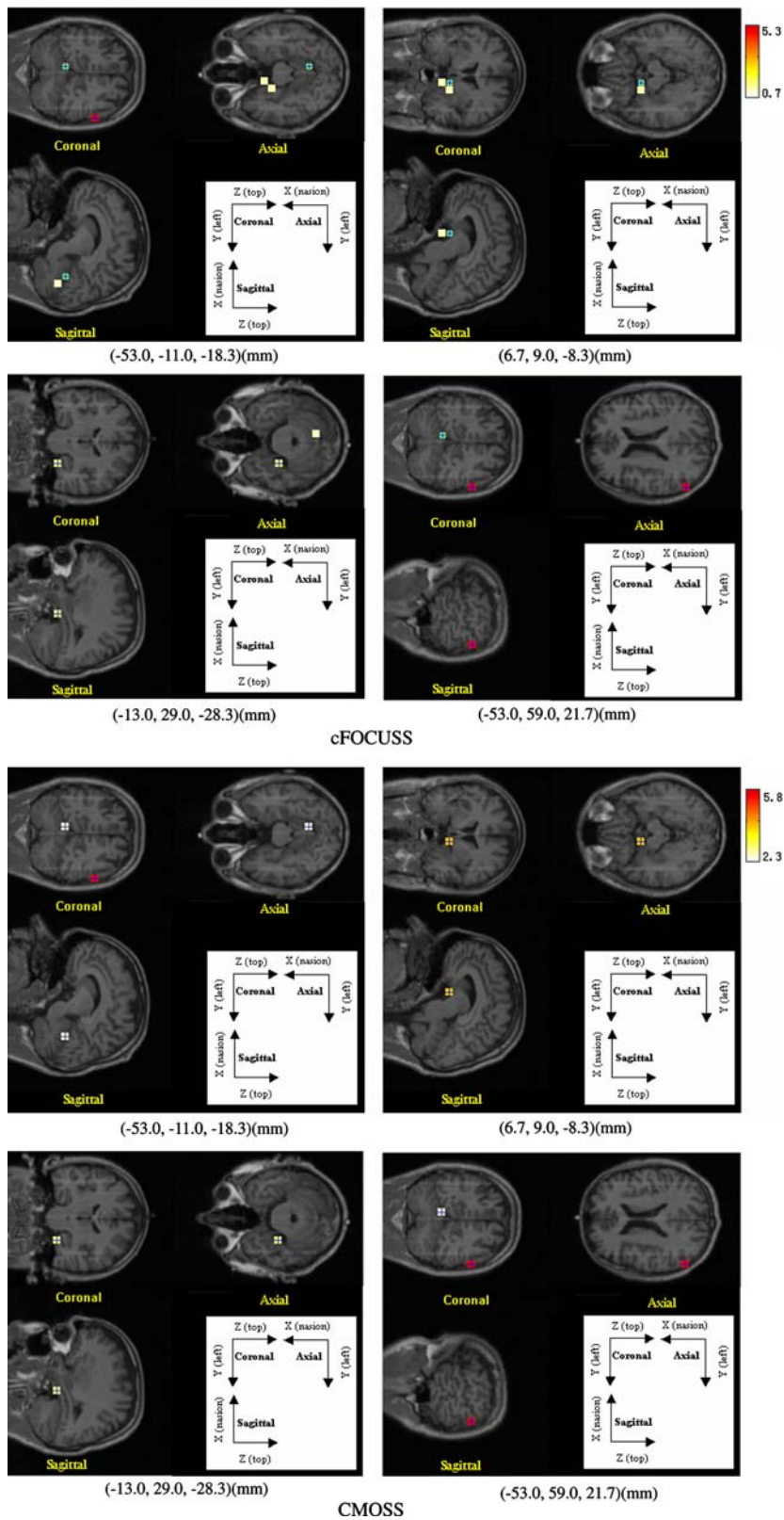


FIGURE 5. continued.

As shown in Fig. 9, the strong activations at 176 ms elicited by the left stimuli were mainly localized in the right occipital (i.e. the contralateral to the visual stimulus), and the left occipital also was weakly

activated. These early sensory related activations reflected that the visual stimulus was perceived in the primary visual cortex. The relatively weak activations were localized in the left frontal eye fields and the right

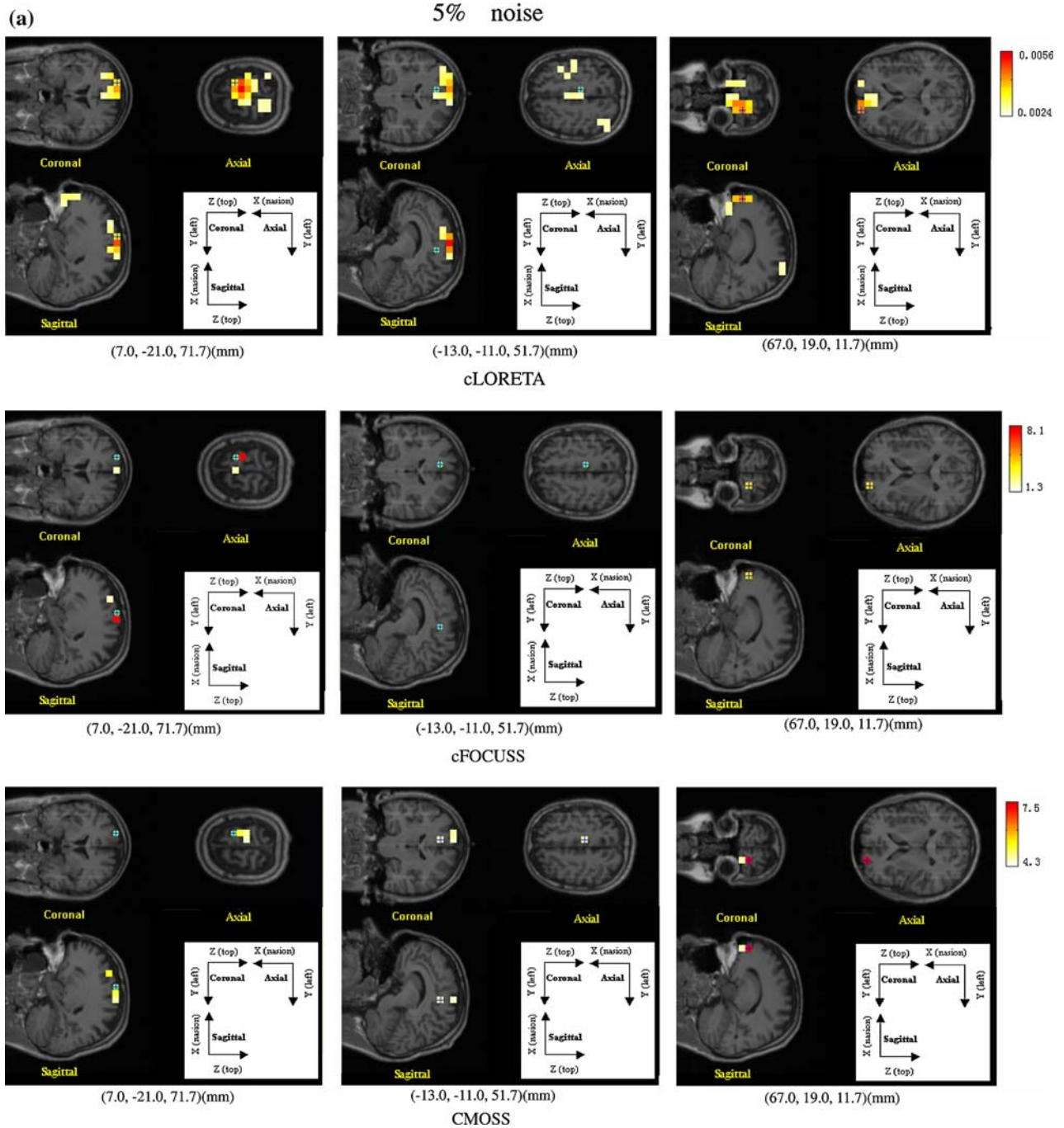


FIGURE 6. Localization for configuration with three sources under noise of different NSRs. Colorful rectangle area in (b) is the estimated source location; the blue cross line within the colorful rectangle area indicates the overlapping area of the simulated source and the estimated source; the blue cross line within green circle indicates those simulated source locations that are not overlapped with the positions of the estimated sources.

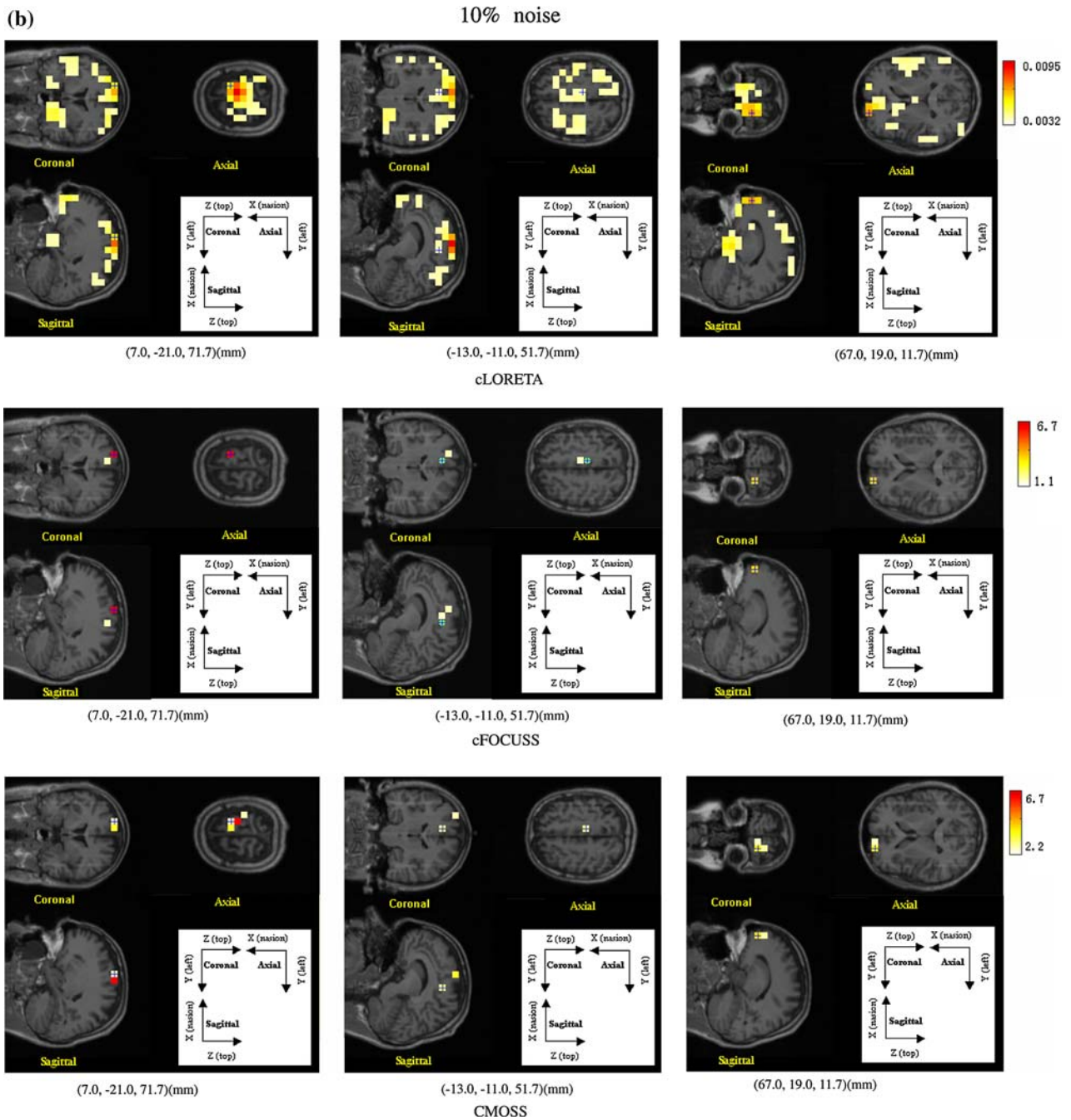


FIGURE 6. continued.

parietal areas. The common activation of these two oculomotor areas were consistently involved in exogenous orienting.<sup>13,14,24,25</sup>

## DISCUSSION AND CONCLUSIONS

In section “Localization for different source configurations,” three different source configurations including the deep sources were used to test the

localization ability of cLORETA, cFOCUSS and CMOSS. For the tested three configurations, cLORETA and cFOCUSS both showed some localization bias toward the superficial surface for the deep sources or even lost them. Furthermore, as shown in Figs. 2a, 3a, and 5a, the source configuration estimated with cLORETA was very scattering and blurring with most sources strength rather weaker than actual they were. Compared with cLORETA, the sources recovered by cFOCUSS were much closer to

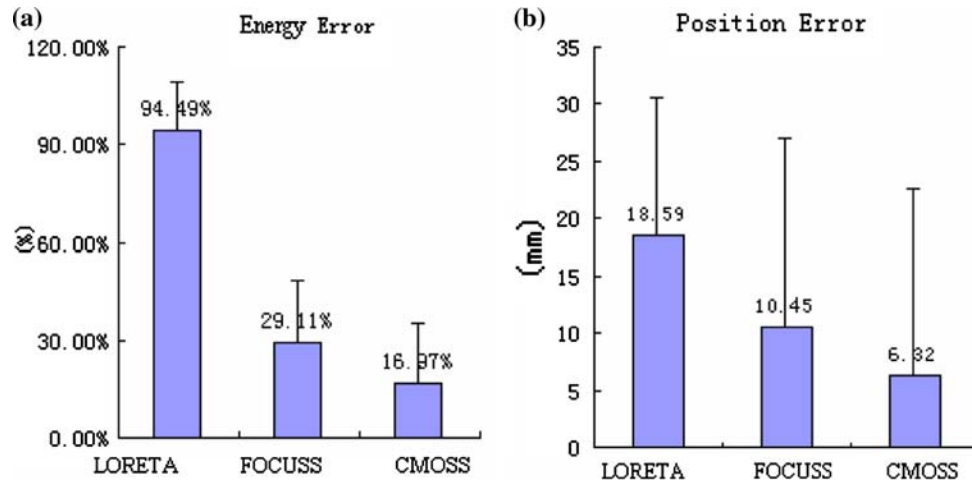


FIGURE 7. The statistical localization indices of cLORETA, cFOCUSS and CMOSS. (a) Mean and SD of  $E_{\text{localization}}$ ; (b) Mean and SD of  $E_{\text{energy}}$ .

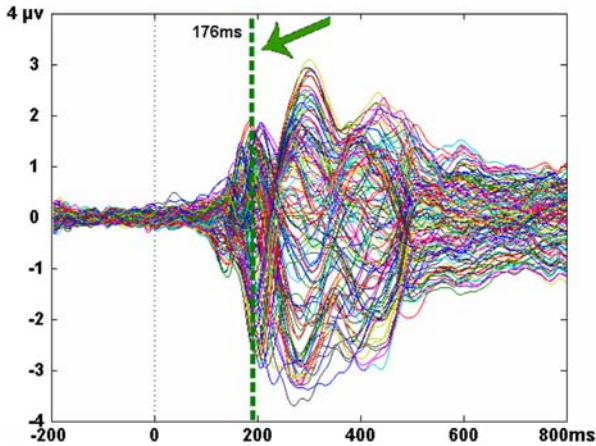


FIGURE 8. ERP evoked by left target stimuli.

the actual cases. For CMOSS and cFOCUSS, there were many cases that both cFOCUSS and CMOSS recovered the actual sources well, which were not reported in this paper. The shown three cases are configurations that cFOCUSS did not recover the sources perfectly, but CMOSS did. When using the new weighting matrix combined with the neighboring source information, CMOSS modified the possible estimation bias and reconstructed the sources ideally. As shown in Fig. 4, the difference between cFOCUSS procedure and CMOSS procedure was obvious: In the iterations of cFOCUSS, only two relatively strong sources were observed. As shown in Fig. 3, cLORETA did not estimate a relatively strong source at the expected solution position for the third source, and when cFOCUSS was initialized with this cLORETA solution, the adopted weight strategy would consistently impose a small weight on this solution point in the following iterations, which would not provide the

strong enough competitive ability for the source on this point to compete with points in the discrete solution space with strong source values. As the iterations show, the cFOCUSS weighting strategy did not effectively modify the bias during iterations and accordingly lost this source eventually. During the iterations based on the new weight matrix, though the source at the simulated source 3 was still of small strength in the first iteration, however, with the combination of neighboring source information into the iterations, a stronger weight than that constructed in cFOCUSS procedure was assigned to this solution point, which would give this point more chance to compete with other positions. With this enhanced weight strategy, the bias could be gradually modified in the following iterations and the source lost in cFOCUSS could be well recovered. As shown in Fig. 4, from the 2th iteration, CMOSS began to construct a relatively strong source on the position of source 3, which was still weak in the corresponding iterations of cFOCUSS. When source configuration becomes more complex with more sources or with deep sources, both cFOCUSS and cLORETA showed to be uncompetitive to image them with some blurring and biased sources occurring,<sup>15,16</sup> however the results in this section confirmed that CMOSS was less affected by the source configurations and could localize those sources robustly.

When contaminated with noise, the sources estimated with cLORETA, cFOCUSS and CMOSS were more blurring with some relatively strong artificial sources occurring in other unexpected positions. Compared with cLORETA and cFOCUSS, CMOSS still recovered the sources with higher accuracy.

For the statistical performance calculated on the whole discrete solution space, the  $E_{\text{localization}}$  and  $E_{\text{energy}}$  of cLORETA were much larger than those

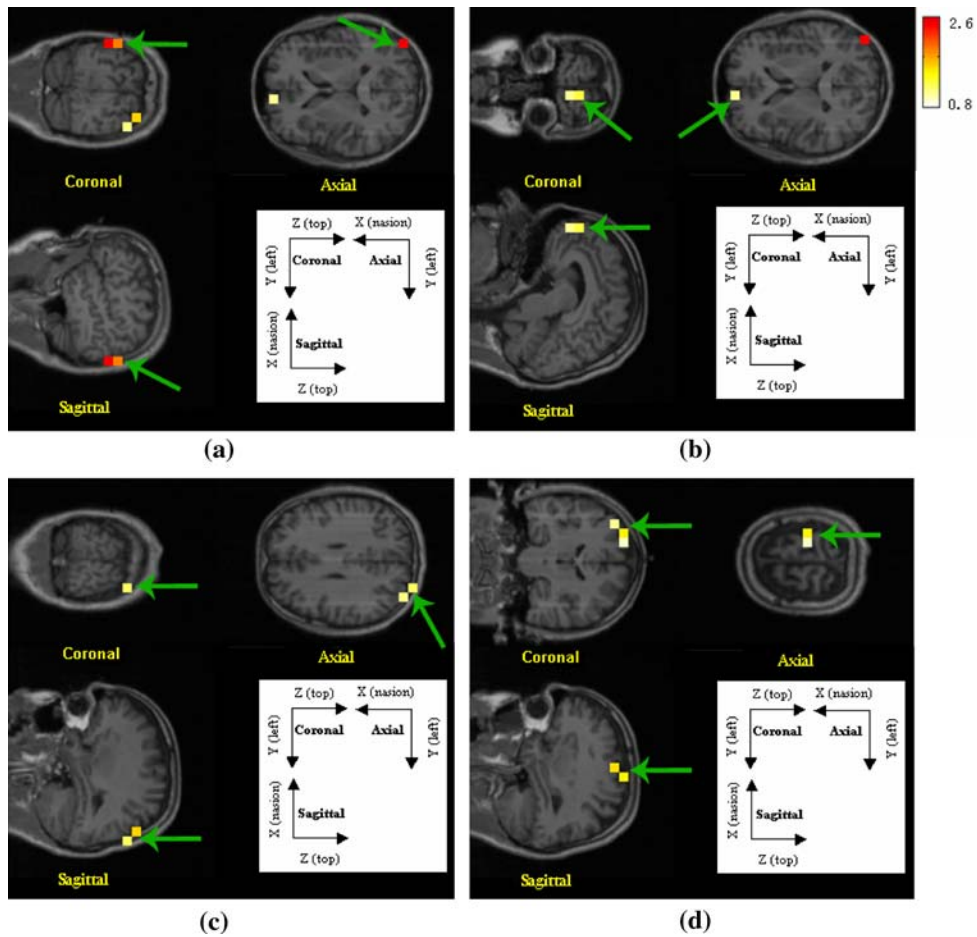


**FIGURE 9.** The activated areas of left visual stimulus localized with CMOSS. Areas tagged with arrows: (a) right occipital; (b) left frontal eyes fields; (c) left occipital; (d) right parietal areas.

calculated with other two methods. However, this result just means cLORETA is not so good for localizing sparse sources. cFOCUSS localized the tested 910 isolated sources well with 10.45 mm for average of  $E_{\text{localization}}$  and 29.11% for average of  $E_{\text{energy}}$ . When CMOSS was used, the average of  $E_{\text{localization}}$  and  $E_{\text{energy}}$  were 6.45 mm, 16.97% for the 910 cases.

When applied to localize the sources elicited by the left visual stimuli, the activations were mainly detected in right occipital, left frontal eyes fields, left occipital and right parietal areas, and these activated areas were consistent with those reported in previous similar visual researches.<sup>13,14,24,25</sup>

In essence, the new weight strategy gives CMOSS more chance to correct the biased solution in the iterations. In the cFOCUSS iteration procedure, once the source on the true position was incorrectly estimated with a rather weak strength in certain iteration step, in the following iterations, this source is easy to be compressed because of the smaller weight imposed on it, and it is very hard for cFOCUSS to modify this bias. Whereas, by combining the neighbor source

information into the new weight, the sources on those points in the solution space incorrectly compressed in previous iteration still have chance to be re-emphasized by the information of neighboring sources, thus those re-emphasized points can compete with other points to capture possible strong sources on them again, and accordingly the possible bias may be compensated in the following iterations.

Certainly, as CMOSS was designed to localize sparse sources, for an actual extensive source configuration, it may not get the real image but an equivalent sparse one with some sources lost just like that of cFOCUSS. In this paper, the inverse problem was solved with the charge source model, and accordingly the similar weighting strategy was suitable for the dipole model or the local field potential model, where the main difference among them is only the different lead fields  $A$  and different number of unknown variables for inverse problem. In this work, we make use of the original version of LORETA to get the initialization values for both FOCUSS and CMOSS, we may also use other new low-resolution solution such as

eLORETA<sup>21</sup> or sLORETA<sup>20</sup> to initialize FOCUSS and CMOSS, and such a substitution may potentially further improve the performance of them.

### ACKNOWLEDGMENTS

This work was supported by NSFC (#30525030, #60701015, #60736029 and #30570474) and the 973 project 2003CB617106 and 2006CB504501.

### REFERENCES

- <sup>1</sup>Cuffin, B. N. Effects of head shape on EEG's and MEG's. *IEEE Trans. Biomed. Eng.* 37(1):44–52, 1990. doi:[10.1109/10.43614](https://doi.org/10.1109/10.43614).
- <sup>2</sup>Fuchs, M., and R. Drenckhahn. An improved boundary element method for realistic volume-conductor modeling. *IEEE Trans. Biomed. Eng.* 45(8):980–997, 1998. doi:[10.1109/10.704867](https://doi.org/10.1109/10.704867).
- <sup>3</sup>George, J. S., P. S. Lewis, H. A. Schlitt, L. Kaplan, I. F. Gorodnitsky, and C. Wood. Strategies for source space limitation in tomographic inverse procedures. In: Proc. 9th Int. Conf. on Biomagnetism. Vienna, Austria, 16–20 Aug, 1993.
- <sup>4</sup>Gorodnitsky, I. F., J. S. George, and B. D. Rao. Neuromagnetic source imaging with focuss: a recursive weighted minimum norm algorithm. *J. Electroencephalogr. Clin. Neurophysiol.* 95(4):231–251, 1995. doi:[10.1016/0013-4694\(95\)00107-A](https://doi.org/10.1016/0013-4694(95)00107-A).
- <sup>5</sup>Gorodnitsky, I. F., and B. D. Rao. A new iterative weighted norm minimization algorithm and its applications. In: Proc. 6th SP Workshop on Statistical Signal and Array Processing, 1992, pp. 412–415.
- <sup>6</sup>Gorodnitsky, I. F., and B. D. Rao. Sparse signal reconstruction from limited data using FOCUSS: a re-weighted minimum norm algorithm. *IEEE Trans. S.P.* 45:600–616, 1997. doi:[10.1109/78.558475](https://doi.org/10.1109/78.558475).
- <sup>7</sup>Grave de Peralta Menendez, R., S. L. Gonzalez Andino, S. Morand, C. M. Michel, and T. Landis. Imaging the electrical activity of the brain: ELECTRA. *Hum. Brain Mapp.* 9:1–12, 2000. doi:[10.1002/\(SICI\)1097-0193\(2000\)9:1<1::AID-HBM1>3.0.CO;2-#](https://doi.org/10.1002/(SICI)1097-0193(2000)9:1<1::AID-HBM1>3.0.CO;2-#).
- <sup>8</sup>Grova, C., J. Daunizeau, J. M. Lina, C. G. Be'nar, H. Benali, and J. Gotman. Evaluation of EEG localization methods using realistic simulations of interictal spikes. *Neuroimage* 29:734–754, 2006. doi:[10.1016/j.neuroimage.2005.08.053](https://doi.org/10.1016/j.neuroimage.2005.08.053).
- <sup>9</sup>Hämäläinen, M. S., and R. J. Ilmoniemi. Interpreting measured magnetic fields of the brain: estimates of current distributions. Helsinki Univ. Technol., Helsinki, Finland, Tech. Rep TKK-F-A559, 1984.
- <sup>10</sup>Hauk, O. Keep it simple: a case for using classical minimum norm estimation in the analysis of EEG and MEG data. *Neuroimage* 21:1612–1621, 2004. doi:[10.1016/j.neuroimage.2003.12.018](https://doi.org/10.1016/j.neuroimage.2003.12.018).
- <sup>11</sup>He, B., D. Yao, J. Lian, and D. Wu. An equivalent current source model and Laplacian weighted minimum norm current estimates of brain electrical activity. *IEEE Trans. Biomed. Eng.* 54(4):222–228, 2002.
- <sup>12</sup>Henderson, C. J., S. R. Butler, and A. Glass. The localization of equivalent dipoles of EEG sources by the application of electrical field theory. *Electroencephalogr. Clin. Neurophysiol.* 39:117–130, 1975. doi:[10.1016/0013-4694\(75\)90002-4](https://doi.org/10.1016/0013-4694(75)90002-4).
- <sup>13</sup>Jonides, J., and D. E. Irwin. Capturing attention. *Cognition* 10:145–150, 1981. doi:[10.1016/0010-0277\(81\)90038-X](https://doi.org/10.1016/0010-0277(81)90038-X).
- <sup>14</sup>Lepsien, J., and S. Pollmann. Covert reorienting and inhibition of return: an event-related fMRI study. *J. Cogn. Neurosci.* 14:127–144, 2002. doi:[10.1162/089892902317236795](https://doi.org/10.1162/089892902317236795).
- <sup>15</sup>Liu, H. S., X. R. Gao, P. H. Schimpf, F. S. Yang, and S. K. Gao. A recursive algorithm for the three-dimensional imaging of brain electric activity: shrinking LORETA-FOCUSS. *IEEE Trans. Biomed. Eng.* 51(10):1794–1802, 2004. doi:[10.1109/TBME.2004.831537](https://doi.org/10.1109/TBME.2004.831537).
- <sup>16</sup>Michel, C. M., M. M. Murray, G. Lantz, S. Gonzalez, L. Spinelli, and R. Grave de Peralta. EEG source imaging. *Clin. Neurophysiol.* 115:2195–2222, 2004. doi:[10.1016/j.clinph.2004.06.001](https://doi.org/10.1016/j.clinph.2004.06.001).
- <sup>17</sup>Murray, J. F., and K. Kreutz-Delgado. An improved Focuss-based learning algorithm for solving sparse linear inverse problems. Signals, Systems and Computers, Conference Record of the 35th Asilomar Conference on 1:4–7, 2001.
- <sup>18</sup>Net Station Viewer Technical Manual. Electrical Geodesics, Inc., 2003, pp. 153–166.
- <sup>19</sup>Nunez, P. L., and R. Srinivasan. Electric Fields of the Brain: The Neurophysics of EEG. 2nd ed. New York: Oxford University Press, pp. 251–275, 2006.
- <sup>20</sup>Pascual-Marqui, R. D. Standardized low resolution brain electromagnetic tomography (sLORETA): technical details. *Methods Find. Exp. Clin. Pharmacol.* 24D:5–12, 2002.
- <sup>21</sup>Pascual-Marqui, R. D. Discrete, 3D distributed, linear imaging methods of electric neuronal activity. Part I: exact, zero error localization. arXiv:0710.3341 [math-ph], October 17, 2007. <http://arxiv.org/pdf/0710.3341>.
- <sup>22</sup>Pascual-Marqui, R. D., C. M. Michel, and D. Lehmann. Low resolution electromagnetic tomography: a new method for localizing electrical activity in the brain. *Int. J. Psychophysiol.* 18:49–65, 1994. doi:[10.1016/0167-8760\(84\)90014-X](https://doi.org/10.1016/0167-8760(84)90014-X).
- <sup>23</sup>Picton, T. W., S. Bentin, P. Berg, E. Donchin, S. A. Hillyard, J. R. Johnson, G. A. Miller, W. Ritter, D. S. Ruchkin, M. D. Rugg, and M. J. Taylor. Guidelines for using human event-related potentials to study cognition: recording standards and publication criteria. *Psychophysiology* 37(2):127–152, 2000. doi:[10.1017/S0048577200000305](https://doi.org/10.1017/S0048577200000305).
- <sup>24</sup>Posner, M. I., R. D. Rafal, L. S. Choate, and J. Vaughan. Inhibition of return: neural basis and function. *Cogn. Neuropsychol.* 2:211–228, 1985. doi:[10.1080/02643298508252866](https://doi.org/10.1080/02643298508252866).
- <sup>25</sup>Ro, T., A. Farne, and E. Chang. Inhibition of return and the human frontal eye fields. *Exp. Brain Res.* 150:290–296, 2003.
- <sup>26</sup>Rush, S., and D. A. Driscoll. EEG electrode sensitivity—an application of reciprocity. *IEEE Trans. Biomed. Eng.* 16:15–22, 1969. doi:[10.1109/TBME.1969.4502598](https://doi.org/10.1109/TBME.1969.4502598).
- <sup>27</sup>Scherg, M., and D. Von Cramon. Evoked dipole source potentials of the human auditory cortex. *Electroencephalogr. Clin. Neurophysiol.* 65:344–360, 1986. doi:[10.1016/0168-5597\(86\)90014-6](https://doi.org/10.1016/0168-5597(86)90014-6).
- <sup>28</sup>Silva, C., J. C. Maltez, and E. Trindade. Evaluation of L<sub>1</sub> and L<sub>2</sub> minimum norm performances on EEG localizations. *Clin. Neurophysiol.* 115:1657–1668, 2004. doi:[10.1016/j.clinph.2004.02.009](https://doi.org/10.1016/j.clinph.2004.02.009).

- <sup>29</sup>Tikhonov, A. N., and V. Y. Arsenin. Solutions of Ill-posed Problems. Trans. from Russian. New York: Wiley, 1977.
- <sup>30</sup>Wang, J. Z., S. J. Williamson, and L. Kaufman. Magnetic source images determined by a lead-field analysis: the unique minimum-norm least-squares estimation. *IEEE Trans. Biomed. Eng.* 39:665–675, 1992. doi:[10.1109/10.142641](https://doi.org/10.1109/10.142641).
- <sup>31</sup>Xu, P., T. Yin, H. F. Chen, and D. Yao. Lp norm iterative sparse solution for EEG source localization. *IEEE Trans. Biomed. Eng.* 54(3):400–409, 2007. doi:[10.1109/TBME.2006.886640](https://doi.org/10.1109/TBME.2006.886640).
- <sup>32</sup>Yao, D. The equivalent source technique and cortical imaging. *Electroencephalogr. Clin. Neurophysiol.* 98:478–483, 1996. doi:[10.1016/0013-4694\(96\)94694-5](https://doi.org/10.1016/0013-4694(96)94694-5).
- <sup>33</sup>Yao, D., and B. He. The Laplacian weighted minimum norm estimated of three-dimensional equivalent charge distribution in the brain. In: 20th Proc. IEEE/EMBS, 1998, pp. 2108–2111.
- <sup>34</sup>Yao, D., and B. He. A self-coherence enhancement algorithm and its application to enhancing 3D source estimation from EEGs. *Ann. Biomed. Eng.* 29(11):1019–1027, 2001. doi:[10.1114/1.1415526](https://doi.org/10.1114/1.1415526).
- <sup>35</sup>Yao, D., L. Wang, K. D. Nielsen, L. Nielsen, and C. N. Andrew. Cortical mapping of EEG alpha power using a charge layer model. *Brain Topogr.* 17(2):65–71, 2004. doi:[10.1007/s10548-004-1004-5](https://doi.org/10.1007/s10548-004-1004-5).
- <sup>36</sup>Yao, D., Z. K. Yin, X. H. Tang, L. Nielsen, and C. N. Andrew. High-resolution electroencephalogram (EEG) mapping: scalp charge layer. *Phys. Med. Biol.* 49:5073–5086, 2004. doi:[10.1088/0031-9155/49/22/004](https://doi.org/10.1088/0031-9155/49/22/004).